Computational and Theoretical Chemistry 965 (2011) 168–175

Contents lists available at ScienceDirect

Computational and Theoretical Chemistry

journal homepage: www.elsevier.com/locate/comptc

Theoretical study on the electronic structure and the absorption spectra of complexes of C_{60} and $C_{59}N$ with π-extended derivatives of tetrathiafulvalene

Ioannis D. Petsalakis, Demeter Tzeli, Ioannis S.K. Kerkines, Giannoula Theodorakopoulos *

Theoretical and Physical Chemistry Institute, The National Hellenic Research Foundation, 48 Vassileos Constantinou Ave., 116 35 Athens, Greece

ARTICLE INFO

Article history:
Received 12 November 2010
Received in revised form 25 January 2011
Accepted 25 January 2011
Available online 1 February 2011

Keywords:
Azafullerene
Fulleropyrrolidine
Supramolecular complexes
Electronic structure
Excited states

ABSTRACT

A theoretical study has been carried out on the ground and the excited electronic states of models of supramolecular complexes of π-extended derivatives of tetrathiafulvalene (exTTF) with fullerene and fulleropyrrolidine, as well as covalently bonded exTTF to fulleropyrrolidine and to azafullerene. Density Functional theory (DFT) and Time Dependent DFT (TDDFT) calculations employing B3LYP, MPWB1K and CAM-B3LYP functionals have been carried out on the above systems in the gas phase as well as in toluene solvent. The lowest 30–50 excited electronic states of these systems have been determined at the ground state optimum geometry. The results show that the exTTF absorption maximum calculated in the hybrid structures is only slightly shifted with respect to that calculated for free exTTF, with the largest red shift found for the hydrogen-bonded exTTF to fulleropyrrolidine complex. In all cases, charge-transfer excitations are found, involving electron excitation from exTTF to fullerene, contributing either to the character of the absorbing state or to that of a nearly-degenerate state.

1. Introduction

Nanohybrid systems involving fullerene as electron acceptor and different fluorophores as electron donors have received considerable interest in the quest for novel materials with desired functionalities for organic photovoltaics and molecular electronics [1]. Conjugates of fullerene with π-extended derivatives of tetrathiafulvalene (exTTF) have been examined, involving either covalent attachment via different spacers [2] or noncovalent binding of exTTF "tweezers" to fullerene [3,4], while a strategy leading to cooperativity between π–π and hydrogen-bonding interactions has been adopted in order to form 1:1 complexes (exTTF:C_{60}) [5]. As with other chromophores, of relevance to the organic photovoltaics and molecular electronics applications is the possible photo-induced charge-transfer from excited exTTF to fullerene and indeed it has been reported that the formation of complexes of exTTF with fullerene are associated with changes in the UV–vis spectra of exTTF consistent with the formation of charge-transfer states [3–5].

In the present work a theoretical study is presented on the ground and excited electronic states of supramolecular complexes of exTTF with C_{60} fullerene and with fulleropyrrolidine, involving physisorption in the former and hydrogen-bonding in the latter, as well as covalently bound complexes of exTTF with fulleropyrrolidine and with azafullerene in order to determine the excited electronic states of the differently-bonded complexes and in particular the character of the electronic states in the vicinity of the exTTF absorption energy. To our knowledge, there have not been any reports of previous theoretical work on the electronic states of exTTF nor on the electronic states of the complexes of $C_{59}N$ azafullerene treated here.

2. Calculations

The systems under consideration in the present work are shown schematically in Fig. 1, where the optimum structures calculated for the ground electronic state in each case (see below) are given. Structure (i), cf. Fig. 1, which involves physisorbed exTTF at C_{60}, is basically a model for the purposes of the calculations, because such a complex has not been formed experimentally in this 1:1 form. Structure (ii) is a model system of a hybrid involving attachment through hydrogen-bonding and it has been constructed by attaching a –COOH group to the α-carbon of fulleropyrrolidine and a corresponding –COOH group replacing one phenyl hydrogen of exTTF. Structures (iii) and (iv) involve covalent bonding, with the exTTF attached to C_{60} via a fused pyrrolidine ring, at the end of a spacer chain and at the α-carbon, respectively. Systems of type (iii) and (iv) have been formed experimentally with other fluorophores [6,7]. Structures (v) and (vi) also involve covalent bonding but in these cases exTTF is bonded at the end of either a short spacer chain (v) or a long chain (vi) attached to a C atom adjacent to the N atom in azafullerene ($C_{59}N$), cf. Fig. 1. These complexes of azafullerene have been recently synthesized [8]. In addition to the

* Corresponding author. Tel.: +30 2107273800; fax: +30 2107273794.
E-mail address: ithe@eie.gr (G. Theodorakopoulos).

2210-271X/$ - see front matter © 2011 Elsevier B.V. All rights reserved.
doi:10.1016/j.comptc.2011.01.041

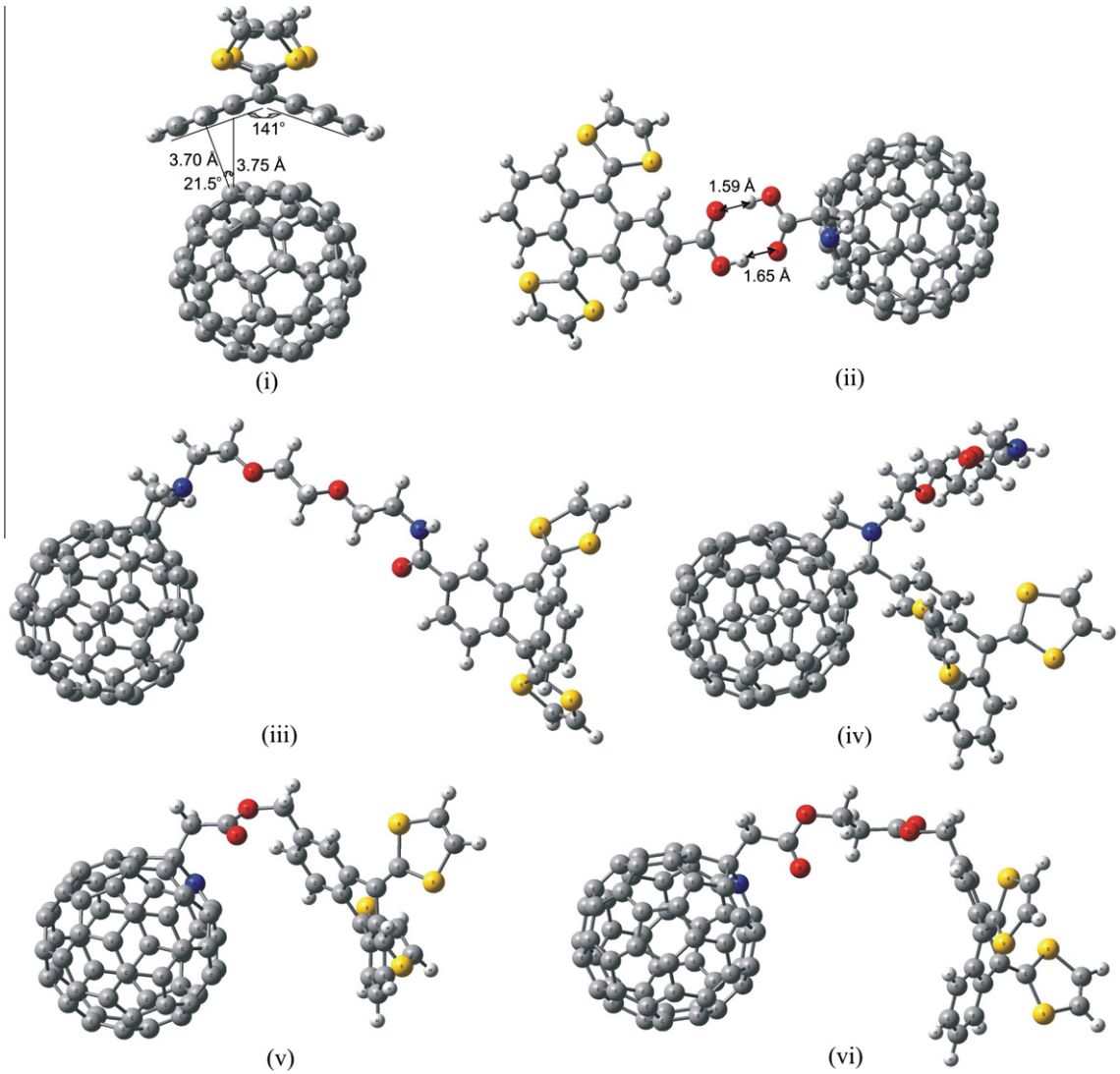

Fig. 1. Optimum geometry of (i) exTTF physisorbed at C_{60} fullerene, (ii) hydrogen-bonded model of exTTF to fulleropyrrolidine, (iii) covalently bonded exTTF to fulleropyrrolidine in the **out** and (iv) **in** structures, and covalently bonded exTTF to azafullerene, with a short (v) and long (vi) spacer chain.

above hybrid structures, calculations on the separate donor and acceptor systems have been also carried out for comparison.

Geometry optimization Density Functional Theory (DFT) [9] calculations have been carried out on the ground electronic state of the aforementioned structures employing three different functionals, B3LYP [10] MPWB1K [11] and CAM-B3LYP [12]. The B3LYP functional is the one most widely used, often very successfully for the determination of equilibrium geometries and excitation energies, especially for strongly bound complexes. However, TDDFT/B3LYP calculations have been reported to underestimate the excitation energies to charge-transfer states [12,13] while the CAM-B3LYP functional has been developed so as to correct for the long-range behavior and is thus considered as more appropriate for calculation of the involvement of the charge-transfer states in the absorption spectra of the complexes [12]. In view of the possible involvement of charge-transfer in the excited electronic states of the different complexes, it is important, to the extent possible, to calculate in a balanced manner the excitations of different characters which are possibly interacting and contributing to the excited electronic states. Thus both B3LYP and CAM-B3LYP functionals have been employed for the calculations. Furthermore, the MPWB1K functional is also commonly used, particularly for weakly bound systems [11], such as model (i) of the present work, for which it was not possible to obtain a minimum energy structure by DFT/B3LYP (see below), and for this reason the MPWB1K functional was also employed in the present work.

Of the systems considered here, see Fig. 1, a minimum energy structure for (i) was achieved by both DFT/MPWB1K and DFT/CAM-B3LYP calculations but not by the DFT/B3LYP calculations. Ground-state geometry optimizations for all the other structures, (ii)–(vi) were carried out by DFT/B3LYP and DFT/CAM-B3LYP calculations with similar results, shown in Fig. 1.

The singlet-spin excited electronic states of the systems (i)–(vi) as well as of the separated components have been calculated by Time Dependent DFT (TDDFT) [14] calculations. The first step in the photoinduced charge-transfer is absorption of radiation by the chromophore, which in the present work is exTTF, and therefore it is required to calculate the excited states up to the absorption energy of exTTF. In the TD-DFT calculations on the different complexes (i)–(vi), it was thus necessary to include a large number of excited states in order to reach the donor (exTTF) absorbing state because there exist many fullerene local excited states at lower excitation energies (details given below). The calculations were carried out for the isolated systems as well as in the presence

of toluene solvent. For comparison with experiment, the solvent CH_2Cl_2 was also included in the calculations on exTTF.

All the calculations were carried out with the aid of Gaussian 09 and Gaussview 05 [15]. The presence of solvent has been included with the aid of the polarized continuum model PCM [16] as implemented in Gaussian 09. This model is the most commonly used for systems of size as those of the present work and is considered to be the most successful for accounting for the solvent effects in DFT and TD-DFT calculations. The basis sets employed are the 6-31G (d,p) and also 6-31G+(d,p), i.e. including diffuse functions.

3. Results and discussion

3.1. Geometry optimization, binding energies

The DFT/B3LYP geometry optimization calculations resulted in the structures (ii)–(vi) given in Fig. 1. As mentioned above, the geometry optimization for the ground state of the physisorbed structure was carried out using the MPWB1K functional and also with the CAM-B3LYP functional. The minimum energy structure determined is as shown by (i) in Fig. 1, with the central six-membered ring of exTTF above a six-membered ring of fullerene, and the closest carbon–carbon distance at 3.7 Å, which is similar to that of the benzene dimer, but considerably longer than the corresponding distance calculated for the exTTF tweezers–fullerene complexes (3.1–3.4 Å) [5]. The binding energy calculated for (i) by DFT/MPWB1K, as the difference in calculated energy of the hybrid and the sum of the energies of the separate parts is 0.25 eV, while the basis set superposition error (BSSE) [17] is calculated as 0.10 eV, yielding a BSSE-corrected binding energy of only 0.15 eV, signifying an extremely weak binding. The DFT/CAM-B3LYP binding energy of (i) is 0.05 eV with a BSSE correction of 0.10 eV, i.e., the minimum energy structure is not bound. The present results on the binding of the physisorbed structure are consistent with experiment, since attempts to form a stable 1:1 exTTF:fullerene complex without any additional stabilizing interaction have been unsuccessful [4]. Nevertheless, structure (i) will be used in what follows as a model physisorbed supramolecular complex for the calculation of the excited electronic states.

The B3LYP and the CAM-B3LYP geometry optimization calculations on the hydrogen-bonded complex lead to similar results and the optimum geometry, see (ii) of Fig. 1, shows two different O–H bond lengths, 1.59 Å and 1.65 Å. This structure is found to have a binding energy of 0.88 eV by DFT/B3LYP (0.83 eV by DFT/CAM-B3LYP). The BSSE calculated for the hydrogen-bonded structure is 0.05 eV, yielding a BSSE-corrected binding energy of 0.83 eV by DFT/B3LYP (0.78 eV by DFT/CAM-B3LYP). Inclusion of toluene solvent results in a binding energy of 0.71 eV (0.66 BSSE corrected) by DFT/CAM-B3LYP. Thus, the hydrogen-bonded model is predicted to be moderately stable.

Details of the optimum geometries of structures (i)–(vi) are provided in Supplementary information.

3.2. Excited states and the absorption spectrum of exTTF

To our knowledge there have not been any previous calculations on the absorption spectrum of exTTF. In Table 1 the results of the TD-DFT calculations by different approaches on the first and second most intense transitions of the exTTF molecule are collected and can be compared to available experimental data, while the calculated absorption spectra are shown in Fig. 2. As shown in Table 1, making use of different functionals leads to differences in the calculated λ_{max} for exTTF. While there is agreement in the general shape of the UV spectra of exTTF calculated with the different functionals (see Fig. 2), the CAM-B3LYP and MPWB1K absorption maxima are shifted to significantly higher energies than those obtained with the B3LYP functional. As shown in Table 1, the most intense absorption peak of exTTF (corresponding to the S_1 state) is calculated by B3LYP (with the basis set including diffuse functions) near 420 nm in the gas phase and 430 nm in toluene, the corresponding MPWB1K λ_{max} being at 370 and the CAM-B3LYP at 365 nm (375 nm in toluene). With all three functionals the S_1 state is characterized by a HOMO → LUMO (i.e. from the highest occupied molecular orbital to the lowest unoccupied molecular orbital) excitation. The experimental λ_{max} of exTTF in dichloromethane is reported at 415 nm [18] while for a tweezers-shaped derivative including two exTTF units in chlorobenzene λ_{max} is reported at 434 nm. As the exact position of λ_{max} will depend on the experimental conditions, the absorption of exTTF is generally reported around 410–440 nm [2–5]. The TDDFT/B3LYP calculations yield λ_{max} values for the lowest energy most intense peak in the presence of solvent of 418 nm (no diffuse functions included in the basis set) and 433 nm (including diffuse functions), which are in good agreement with the above experimental values.

Table 1
Excitation energies (ΔE), absorption maxima (λ_{max}), oscillator strengths (f-value), and the main excitations contributing to the excited state, for the lowest two absorbing states of exTTF (S_1 and S_3).

Functional, basis set[a], solvent[a]	ΔE (eV)	λ_{max} (nm)	f-value	Excitations
B3LYP, S_1	3.05	406	0.32	H → L
B3LYP, tol, S_1	2.96	418	0.43	H → L
B3LYP, diff, S_1	2.95	420	0.32	H → L
B3LYP, diff, tol, S_1	2.87	433	0.44	H → L
MPWB1K, diff, S_1	3.35	370	0.41	H → L
CAM- B3LYP, diff, S_1	3.43	362	0.44	H → L
CAM-B3LYP, diff, tol, S_1	3.32	374	0.58	H → L
B3LYP, S_3	3.59	345	0.13	H − 1 → L, H → L + 1
B3LYP, tol, S_3	3.52	352	0.19	H − 1 → L, H → L + 1
B3LYP, diff, S_3	3.47	357	0.13	H − 1 → L, H → L + 1
B3LYP, diff, tol, S_3	3.40	365	0.18	H − 1 → L, H → L + 1
MPWB1K, diff, S_3	3.89	318	0.18	H − 1 → L, H → L + 1
CAM- B3LYP, diff, S_3	3.96	313	0.17	H − 1 → L, H → L + 1
CAM-B3LYP, diff, tol, S_3	3.82	324	0.17	H − 1 → L, H → L + 1

[a] tol stands for inclusion of toluene solvent, diff stands for inclusion of diffuse functions in the basis set.

In addition to the λ_{max} of the most intense absorption, in Table 1 data are also included for the second most intense peak of exTTF, corresponding to excitation to the third singlet excited state (S_3), which is characterized by two excitations, HOMO-1 → LUMO and HOMO → LUMO + 1. The value of λ_{max} corresponding to transitions from the ground state to S_3 calculated by TDDFT/B3LYP at 365 nm in toluene, is in good agreement with the reported λ_{max} values ranging from 366 nm to 382 nm in different complexes involving exTTF [4]. Again with CAM-B3LYP and MPWB1K functionals the calculated λ_{max} of the second most intense transition are similar and at higher energy than those obtained with B3LYP (see Table 1). The above results show that for the excited states of exTTF the B3LYP functional leads to λ_{max} values closer to the experimental than the CAM-B3LYP and the MPWB1K. Finally, calculations on exTTF including CH_2Cl_2 as solvent instead of toluene gave identical results as with toluene.

3.3. Physisorbed and hydrogen-bonded systems

Concepts of HOMO–LUMO gaps and electron density pictures are commonly used to rationalize different properties of nanohybrids as well as energy transfer and charge-transfer processes [19]. It is also instructive to compare the orbital energies of the separate systems and those of the complex, for more than just the HOMO and the LUMO, as the near degeneracy of the possible

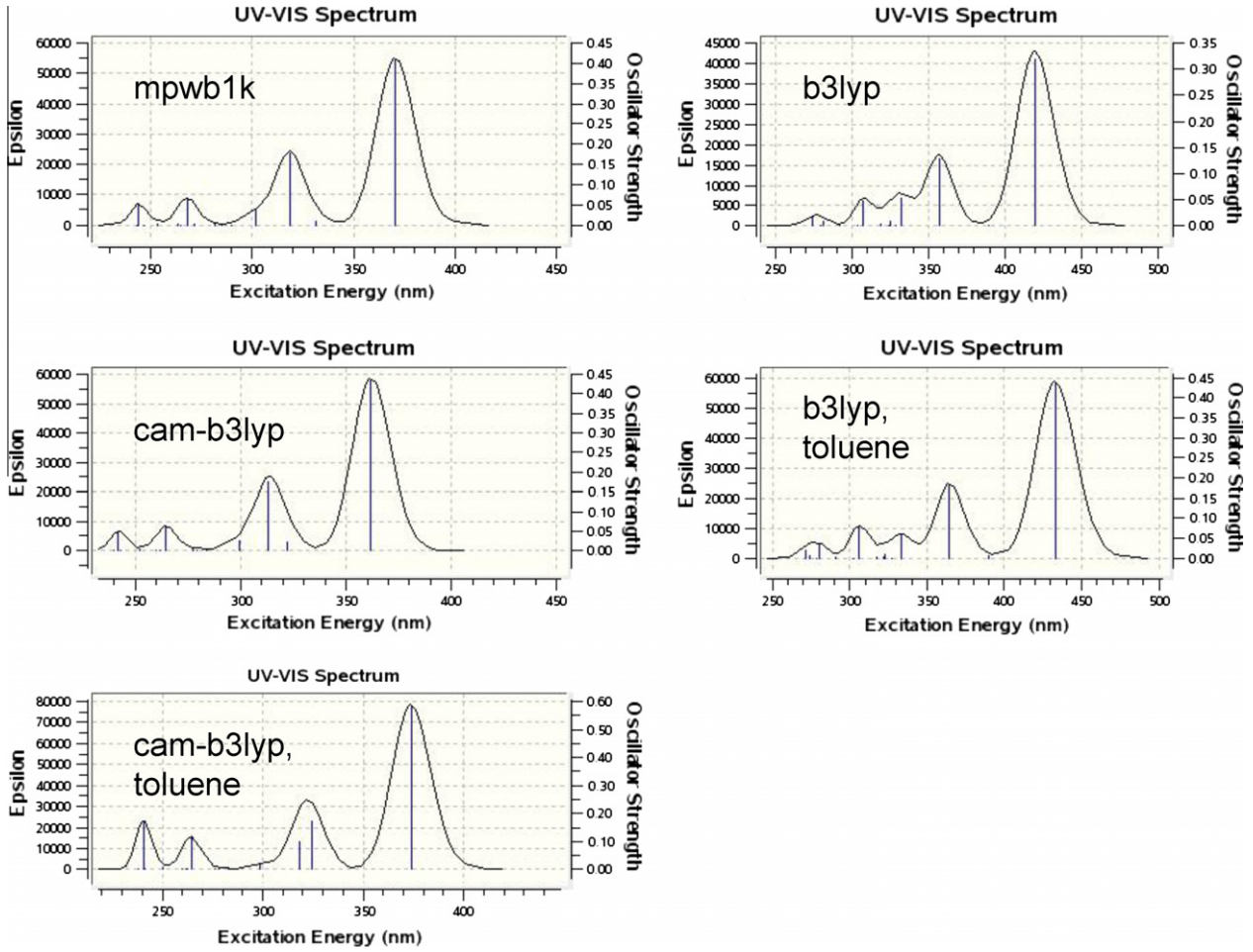

Fig. 2. Absorption spectrum of exTTF calculated with the 6-31G+(d,p) basis set and the different functionals, MPWB1K, CAM-B3LYP and B3LYP isolated and CAM-B3LYP and B3LYP in toluene. The experimental most intense peak is found at 410–440 nm [2–5].

excitations signifies the possibility of corresponding interactions in the excited states [20]. In Fig. 3, orbital levels of exTTF, fullerene and those of the physisorbed complex (i) calculated by DFT/B3LYP (at the MPWB1K geometry) are given. As shown, the orbital levels are not shifted substantially in the complex compared to the separated molecules. Moreover, it is possible to identify excitations which are of charge-transfer character (see D–A* excitation in Fig. 3), since they involve transitions from the occupied orbitals of exTTF (e.g. HOMO-1 of the complex) to some unoccupied orbital of fullerene, with similar excitation energy as the exTTF absorption or D–D* excitation. The possible near degeneracy of the electronic states characterized by the (nearly-degenerate) D–D* and D–A* excitations can lead to interactions and mixing of character of the excited states, possibly accompanying geometrical relaxation in the excited states. In this manner, qualitative conclusions may be drawn on the possibility of photoinduced electron transfer in the complex.

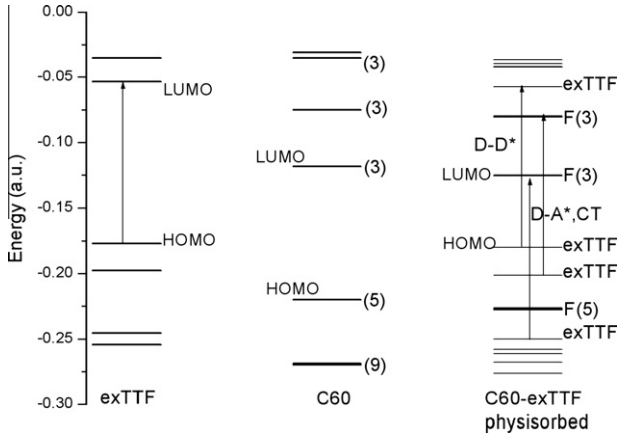

Fig. 3. Orbital level diagram for exTTF, fullerene and the physisorbed exTTF-fullerene complex calculated by DFT/B3LYP/6-31G+(d,p) at the MPWB1K geometry. The numbers in brackets give the degeneracy of the level.

As noted above for exTTF, the use of different functionals results in different calculated transition energies. This is also found for the excited states of fullerene C_{60}: TDDFT/B3LYP calculations carried out on the singlet excited states of isolated fullerene yield the lowest singlet state at 2.09 eV (previously found at 1.94 eV [21]) in very good agreement with the experimental gas phase value of 1.936 eV (~15,616 cm^{-1}) [22]. For comparison, coupled cluster calculations on the electronic states of isolated fullerene, and more specifically calculations employing the resolution-of-identity perturbative corrected coupled cluster doubles, RI-CC2 method [23], and a def2-SVP basis set (employing TURBOMOLE [24]), which is analogous to the basis sets employed in the other calculations of the present work, yield the $S_0 \rightarrow S_1$ transition energy at 2.07 eV, i.e. nearly identical to the TDDFT/B3LYP value. Conversely, TDDFT/CAM-B3LYP calculations result in excitation energy of 2.60 eV for the S_1 state of isolated fullerene, i.e. higher than the B3LYP value by 0.51 eV. As will be seen below, this appears to be a systematic trend for the systems calculated in the present work,

with TDDFT/CAM-B3LYP calculations, and TDDFT/MPWB1K calculations on complex (i), resulting in higher excitation energies than TDDFT/B3LYP, by 0.4–0.7 eV for the electronic states of interest.

The excited electronic states of relevance to the photoinduced charge-transfer process from the exTTF to fullerene following the absorption of light by exTTF, are those calculated in the vicinity of the absorption transition in exTTF. In Table 2, the results of the TD-DFT calculations on the supramolecular complexes (i) and (ii) are summarized. As shown in Table 2, when the physisorbed complex (i) is calculated by TDDFT/B3LYP, at the DFT/MPWB1K minimum energy geometry, the intense exTTF absorption transition (HOMO → LUMO in exTTF) is obtained as an excitation to a higher-lying state characterized mostly by the HOMO → LUMO + 6 excitation. With the MPWB1K and CAM-B3LYP functionals, in the absence of solvent, a significant secondary contribution to the particular excited state is obtained, namely the HOMO → LUMO + 3. Orbital electron density plots show that the HOMO → LUMO + 6 excitation is of D → D* type as expected (i.e. exTTF absorption) but the HOMO → LUMO + 3 is of D → A* type, i.e. of charge-transfer character. With TDDFT/B3LYP, D → A* type excitations are found to characterize electronic states calculated at energies below and just above the D → D* absorbing state. Thus in this case, the interaction of the absorbing and the charge-transfer state and the mixing of their character might occur subsequently to the absorption step, for example, as a result of the geometry relaxation of the excited state [20]. Making use of the B3LYP functionals yields lower transition energy than the values obtained with the other functionals (see Table 2) while very small shifts are calculated for the absorption maxima in the complex (i) with respect to free exTTF (cf. Table 1), within calculations employing the same functional.

The TD-DFT calculations on the hydrogen-bonded complex of exTTF to fulleropyrrolidine, (ii), cf. Table 2, yield again different types of contribution of the charge-transfer character to the excited state of interest, depending on the functional and on the inclusion of the solvent: with B3LYP the exTTF absorbing state is calculated at 468 nm and has mixed D → D* and D → A* character. Inclusion of toluene results in separate absorbing and charge-transfer states with the absorption λ_{max} value calculated at 482 nm. These results are illustrated in Fig. 4, where electron density plots are given for the molecular orbitals involved in these

Table 2
Excitation energies (ΔE), absorption maxima (λ_{max}), oscillator strengths (f-value), main excitations and their coefficient (coeff) contributing to the exTTF absorption excited state in the physisorbed C_{60}-exTTF cluster (i) and the hydrogen-bonded fulleropyrrolidine-exTTF cluster, (ii).

System, functional, basis set[a], solvent[a]	ΔE (eV)	λ_{max} (nm)	f-value	Excitations (coeff)
(i) B3LYP	3.03	409	0.27	H → L + 6 (0.92)
(i) B3LYP, diff	2.93	423	0.25	H → L + 6 (0.91)
(i) B3LYP, tol	2.95	420	0.38	H → L + 6 (0.93)
(i) MPWB1K, diff	3.29	376	0.30	H → L + 3 (0.40)
				H → L + 6 (0.81)
(i) CAM-B3LYP, diff	3.39	365	0.36	H → L + 3 (0.16)
				H → L + 6 (0.96)
(i) CAM-B3LYP, diff, tol	3.30	376	0.49	H → L + 5 (0.96)
(ii) B3LYP	2.65	468	0.15	H − 7 → L (0.26)
				H → L + 5 (0.76)
				H → L + 6 (0.46)
				H → L + 7 (0.17)
(ii) B3LYP, tol	2.57	482	0.25	H → L + 5 (0.95)
(ii) CAM-B3LYP, diff	3.20	388	0.38	H → L + 6 (0.96)
(ii) CAM-B3LYP, diff, tol	3.10	401	0.52	H → L + 5 (0.81)
				H → L + 6 (0.52)

[a] tol stands for inclusion of toluene solvent, diff stands for inclusion of diffuse functions in the basis set.

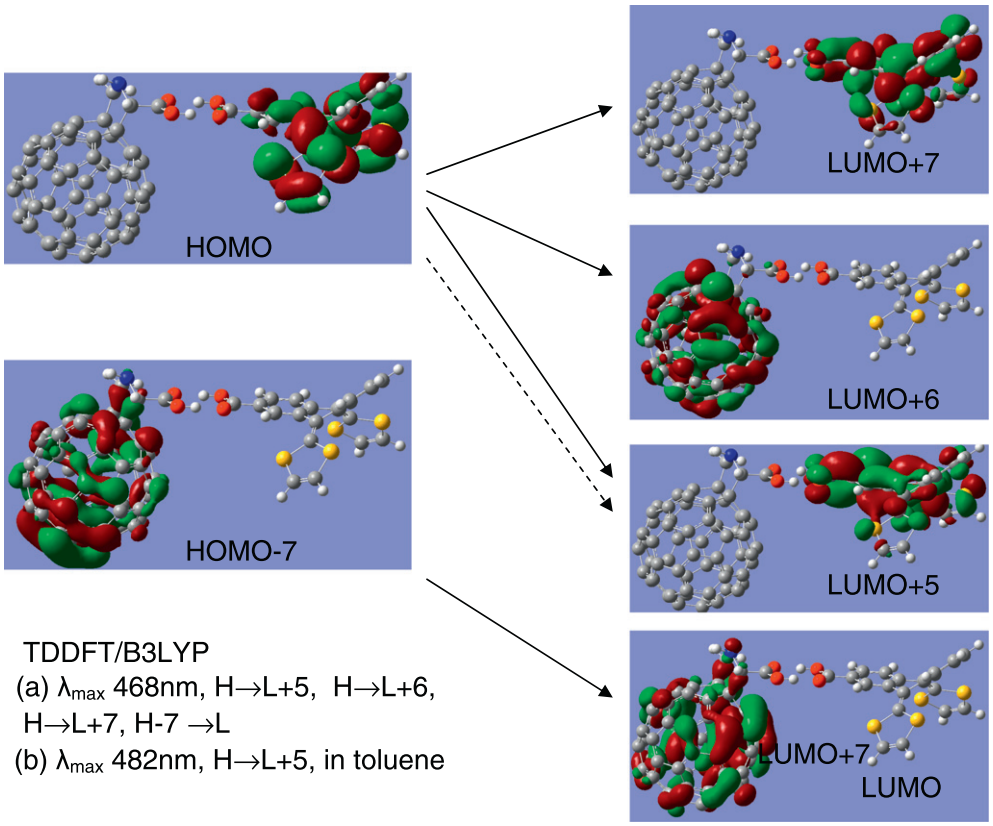

Fig. 4. Electron density plots of the frontier orbitals (6-31G (d,p) basis set) of the hydrogen-bonded complex of exTTF with fulleropyrrolidine, (ii), involved in the exTTF absorption: (a) isolated system (solid arrows) and (b) in toluene (dashed arrow).

$D \rightarrow D^*$ and $D \rightarrow A^*$ excitations. A significant red shift of the exTTF λ_{max} value with respect to the free exTTF is found, for example a λ_{max} of 482 nm for (ii) in toluene compared to 418 nm of free exTTF in toluene (see Table 1). A reduction in the intensity of the absorption peaks is also found, cf. oscillator strength of 0.43 of exTTF with 0.25 of (ii) in toluene.

The TDDFT/CAM-B3LYP calculations on (ii) (see Table 2) result in separate but close-lying absorbing (at 388 nm) and charge-transfer states in the gas phase complex, whereas in toluene a mixed character $D \rightarrow D^*$ and $D \rightarrow A^*$ is obtained for the absorbing state at λ_{max} 401 nm, again calculated at higher energies, in this case by 80 nm (0.5 eV), compared to the B3LYP results. Furthermore with TDDFT/CAM-B3LYP no intensity reduction is found and a smaller red shift in the λ_{max} than that obtained by TDDFT/B3LYP (cf. Table 2).

3.4. Covalently bonded fullerene- and azafullerene-exTTF systems

The results of the TD-DFT calculations on systems (iii) and (iv) are presented in Table 3. As discussed above, structures (iii) and (iv) of Fig. 1, involve covalent attachment of exTTF via a fused pyrrolidine ring to fullerene, either at the end of the connecting triethylene glycol (abbreviated as TEG) chain ((iii) or **out**) or at the α-C atom of the pyrrolidine moiety ((iv) or **in**). Analogous structures have been calculated previously with different fluorophores attached to either fullerene or a nanohorn model, via a fused pyrrolidine ring [21,25]. These systems are large and the calculations are very time-consuming, especially because a very large number of excited states need to be calculated to reach the absorbing exTTF state. In addition, calculations including diffuse functions in the basis set are often difficult to converge and this was the case for the covalently bonded systems with the B3LYP functional and similarly it was impossible to converge the calculation on structure (iv) in toluene with the CAM-B3LYP functional. Thus, the results presented in Table 3 have been obtained with diffuse functions in the basis set in the case of CAM-B3LYP, but without these in the case of B3LYP. Since inclusion of diffuse functions in the case of exTTF leads to lower excitation energies (cf. Table 1), it is expected that including them in the B3LYP calculations would lower even further the B3LYP transition energies. As shown in Table 3, a small red shift is found in the absorption maximum of the **out** system, (iii), compared to free exTTF while the **in** system, (iv), has practically identical absorption λ_{max} as free exTTF, i.e. similar to those calculated for the physisorbed complex (i), cf. Table 2. The λ_{max} values calculated for the **out** system are closer to the experimental values for different hybrid systems involving exTTF. Finally, the CAM-B3LYP maxima for systems (iii) and (iv) are found at higher energies, by about 0.44 eV, than the B3LYP.

Excitations of $D \rightarrow A^*$ type are found to contribute directly to the absorbing state in all the calculations on the **in** structure, and in the B3LYP calculation of the isolated **out** structure. For the **out** structure calculated by B3LYP in toluene, and calculated by CAM-B3LYP isolated as well as in toluene (see Table 3), such excitations characterize separate states, lying very close to the $D \rightarrow D^*$ state and the charge-transfer process possibly occurs as interaction of the absorbing state with a nearly-degenerate charge-transfer state. The size of these systems but especially the fact that the states of interest are highly excited (see root numbers in Table 3) does not allow geometry optimization calculations of the excited states of interest, in the course of which, the interaction of the absorbing state with the charge-transfer state may be revealed (cf. [20]).

The final systems to be discussed are structures (v) and (vi), involving attachment of exTTF via a short or a long chain, respectively, to azafullerene. These systems are of interest especially with regard to the photoinduced charge-transfer process, since azafullerene is considered to be an even better electron acceptor than fullerene. In general, heteroatom-doped carbon conjugated-materials (CCMs) are of current research interest, including DFT/B3LYP calculations [26] as materials of unique properties and potential for applications.

Table 3
Excitation energies (Δ*E*), exTTF absorption maxima (λ_{max}), oscillator strengths (*f*-value), main excitations and their coefficient (coeff) contributing to the excited state, for covalently bonded exTTF to fulleropyrrolidine, structures (iii) and (iv).

System, functional, basis set[a], solvent[a], root no	Δ*E* (eV)	λ (nm)	*f*-value	Excitations (coeff)
(iii) B3LYP, S_{25}	2.90	428	0.26	H → L + 6 (0.91) H → L + 8 (0.14)
(iii) B3LYP, tol, S_{24}	2.80	443	0.37	H → L + 6 (0.93)
(iii) CAM-B3LYP, diff, S_{17}	3.34	371	0.43	H → L + 6 (0.98)
(iii) CAM-B3LYP, diff, tol, S_{16}	3.23	384	0.57	H → L + 6 (0.96)
(iv) B3LYP, S_{28}	3.06	406	0.17	H → L + 6 (0.33) H → L + 7 (0.89)
(iv) B3LYP, tol, S_{27}	2.96	419	0.26	H → L + 5 (0.17) H → L + 6 (0.61) H → L + 7 (0.72)
(iv) CAM-B3LYP, diff, S_{19}	3.40	365	0.38	H → L + 5 (0.34) H → L + 6 (0.25) H → L + 7 (0.86)

[a] tol stands for inclusion of toluene solvent, diff stands for inclusion of diffuse functions in the basis set.

Table 4
Excitation energies (Δ*E*), exTTF absorption maxima (λ_{max}), oscillator strengths (*f*-value), main excitations and their coefficient (coeff) contributing to the excited state, for covalently bonded exTTF to $C_{59}N$ structures (v) and (vi).

System, functional, basis set[a], solvent[a], root no	Δ*E* (eV)	λ (nm)	*f*-value	Excitations (coeff)
(v) B3LYP, S_{29}	3.00	413	0.30	H → L + 6 (0.92)
(v) B3LYP, tol, S_{27}	2.92	425	0.39	H → L + 6 (0.93)
(v) B3LYP, tol, S_{51}[b]	3.47[b]	357[b]	0.21[b]	
(v) CAM-B3LYP, diff, tol, S_{20}	3.40	365	0.54	H → L + 2 (0.16) H → L + 6 (0.95)
(vi) B3LYP, S_{29}	2.99	414	0.30	H → L + 6 (0.92)
(vi) B3LYP, tol, S_{27}	2.90	427	0.42	H → L + 6 (0.93)
(vi) B3LYP, S_{45}[b]	3.45[b]	359[b]	0.23[b]	
(vi) CAM-B3LYP, diff, tol, S_{20}	3.39	366	0.58	H → L + 6 (0.96)

[a] tol stands for inclusion of toluene solvent, diff stands for inclusion of diffuse functions in the basis set.
[b] Second-intense absorption maximum of exTTF.

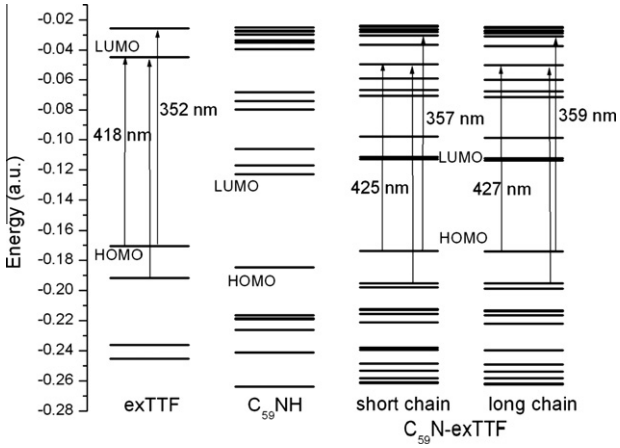

Fig. 5. DFT/B3LYP/6-31G (d,p) orbital level diagram for exTTF, azafullerene and exTTF-azafullerene with short and long spacer in toluene. Arrows indicate the excitations corresponding to the two most intense peaks in the absorption spectrum of exTTF and the numbers are the corresponding TDDFT/B3LYP/6-31G (d,p) λ_{max} in toluene.

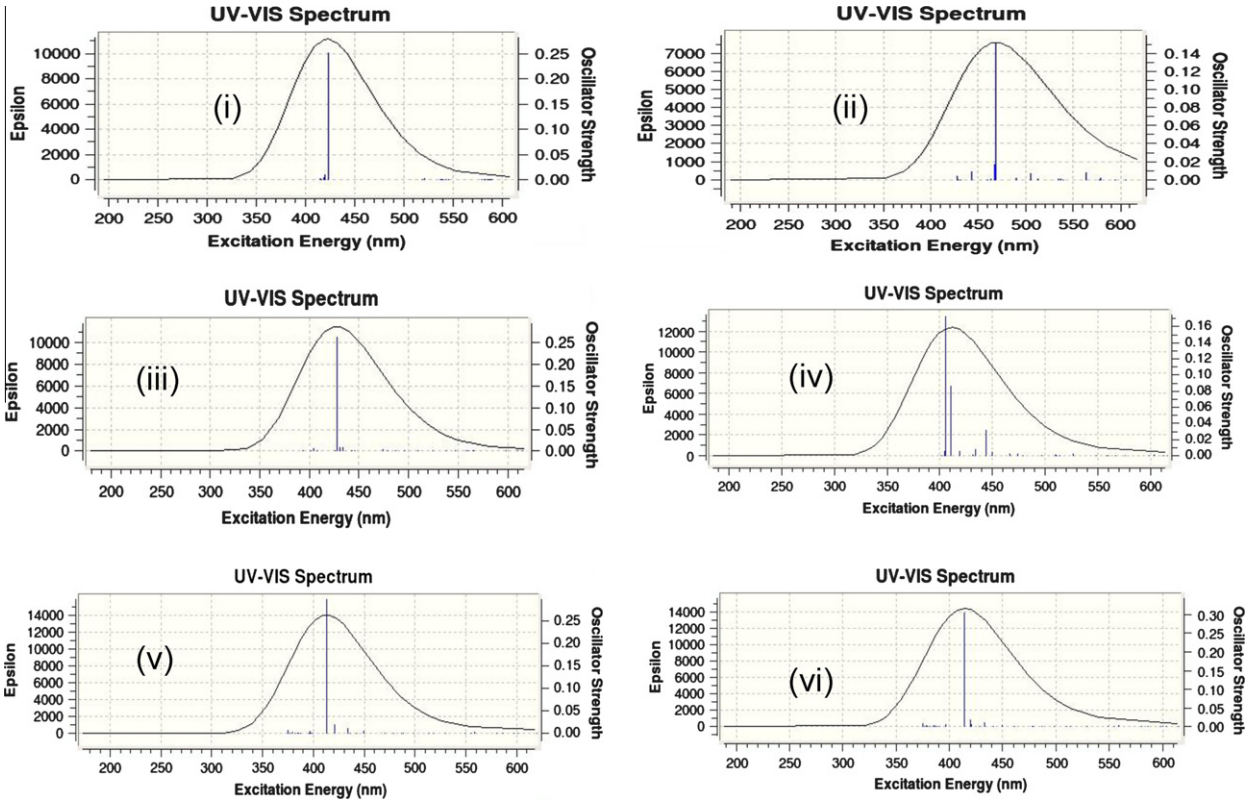

Fig. 6. TDDFT/B3LYP absorption spectra of the different complexes calculated using the 6-31G+(d,p) for (i) and 6-31G (d,p) basis set for complexes (ii)–(vi).

The results of the present TD-DFT calculations on systems (v) and (vi) are summarized in Table 4, where in the B3LYP results the second exTTF intense transition is included in addition to the most intense. In Fig. 5, the orbital level diagram for the separate systems and the complexes (v) and (vi) are shown, where the relevant excitations are shown with values λ_{max} obtained by DFT/B3LYP calculations. What is immediately obvious from the results on systems (v) and (vi) (see Table 4 and Fig. 5) is the fact that the calculations obtain nearly identical λ_{max} for the short-chain and long-chain structures and very close to those of free exTTF (see Table 1), in contrast to the hydrogen-bonded complex (ii). Again, the blue shift of the CAM-B3LYP λ_{max} with respect to the B3LYP is noted. In the complexes of $C_{59}N$ with exTTF the absorbing excited state for the most intense transition is mainly characterized by the $D \rightarrow D^*$, while $D \rightarrow A^*$ excitations characterize different close-lying electronic states.

The calculated (TDDFT/B3LYP in the absence of solvent) absorption spectra of all complexes (i)–(iv) are plotted in Fig. 6, showing very slight shifts in the absorption λ_{max} of the most intense peak in the different complexes with respect to free exTTF. Only for the hydrogen-bonded complex of exTTF to fulleropyrrolidine, (ii), a significant red shift in λ_{max} is found as well as a significant reduction in intensity. A reduction in intensity is also predicted for the exTTF-azafullerene complex, (iv), as shown by the *f*-values in Fig. 6.

4. Conclusions

A theoretical investigation has been presented on the ground and the excited electronic states of two supramolecular complexes of exTTF, one with fullerene and physisorbed exTTF and one with fulleropyrrolidine bound by hydrogen-bonding, as well as covalently bonded exTTF to fulleropyrrolidine and to azafullerene, in an effort to determine how the different modes of binding might affect the absorbing states of exTTF in the complexes and the possibility of photoinduced charge-transfer. The calculated absorption λ_{max} values are not far from those of free exTTF in all types of hybrids considered, except for the hydrogen-bonded exTTF-fulleropyrrolidine structure, where a significant red shift is found. In the different complexes, charge-transfer excitations are found to contribute either directly to the absorbing state or to states close to it possibly interacting with the absorbing state as a result of geometry relaxation. However, because of the large size of the complexes and the fact that the relevant states are high-lying roots, it is not possible to carry out the geometry optimization calculations on these excited states. In this manner, the photoinduced charge-transfer process in these systems may be rationalized only qualitatively, in terms of configuration interaction of the absorbing excitation with a charge-transfer one.

For the systems calculated here, the CAM-B3LYP excitation energies are almost systematically higher than the corresponding B3LYP ones, and in worse agreement with the available experimental data. This result cannot be generalized without further systematic studies on different systems, where the applicability of the different functionals in different situations may be evaluated. For the excited states calculated in the present work, the good performance of the B3LYP functional shows that at the ground-state geometry, relevant to absorption, the charge-transfer contribution is not significant.

Acknowledgments

Financial support from the EU FP7, Capacities Program, NANOHOST Project (GA 201729) and from NATO (Grant No. SPS/CBP.MD.CLG.983711) is acknowledged. The authors are grateful to Dr. N. Tagmatarchis and Dr. G. Rotas for fruitful discussions.

Appendix A. Supplementary material

Supplementary data associated with this article can be found, in the online version, at doi:10.1016/j.comptc.2011.01.041.

References

[1] D.M. Guldi, B.M. Illescas, C.M. Atienza, M. Wielopolski, N. Martín, Chem. Soc. Rev. 38 (2009) 1587.
[2] C.M. Atienza, N. Martin, D.M. Guldi, Chem. Commun. (2009) 5374.
[3] R. Viruela, E. Orti, M. Bietti, N. Martin, Chem. Commun. (2008) 4567.
[4] S.S. Gayarthi, M. Wielopolski, E.M. Pérez, G. Fernádez, L. Sánchez, R. Viruela, E. Orti, D.M. Guldi, N. Martin, Angew. Chem. Int. Ed. 48 (2009) 815.
[5] J. Santos, B. Grimm, B.M. Illescas, D.M. Guldi, N. Martin, Chem. Commun. (2008) 5993;
B.M. Illescas, J. Santos, M.C. Díaz, N. Martin, C.M. Atienza, D.M. Guldi, Eur. J. Org. Chem. (2007) 5027.
[6] N. Tagmatarchis, M. Prato, Synlett (2003) 768;
N. Tagmatarchis, M. Prato, Organofullerene Mater. Struct. Bond. 109 (2004) 1.
[7] D. Benne, E. Maccallini, P. Rudolf, C. Sooambar, M. Prato, Carbon 44 (2006) 2896.
[8] N. Tagmatarchis, G. Rotas, private communication.
[9] R.G. Parr, W. Yang, Annu. Rev. Phys. Chem. 46 (1995) 701.
[10] A.D. Becke, J. Chem. Phys. 98 (1993) 5648;
C. Lee, W. Yang, R.G. Parr, Phys. Rev. B. 37 (1989) 785.
[11] Y. Zhao, D.G.J. Truhlar, Chem. Theory Comput. 4 (2008) 1849;
Y. Zhao, N.E. Schultz, D.G.J. Truhlar, Chem. Theory Comput. 2 (2006) 364;
Y. Zhao, D.G.J. Truhlar, Phys. Chem. A 110 (2006) 5121;
Y. Zhao, D.G. Truhlar, Phys. Chem. Chem. Phys. 7 (2005) 2701;
Y. Zhao, D.G.J. Truhlar, Phys. Chem. A 108 (2004) 6908.
[12] M.J.G. Peach, P. Benfield, T. Helgaker, D.J.J. Tozer, Chem. Phys. 128 (2008) 044118;
T. Yanai, D. Tew, N. Handy, Chem. Phys. Lett. 393 (2004) 51.
[13] T. Stein, L. Kronik, R. Baer, J. Am. Chem. Soc. 131 (2009) 2818.
[14] M.A.L. Marques, E.K.U. Gross, Annu. Rev. Phys. Chem. 55 (2004) 427.
[15] Gaussian 09, Revision A. 1. M.J. Frisch, G.W. Trucks, H.B. Schlegel, G.E. Scuseria, M.A. Robb, J.R. Cheeseman, J.A. Montgomery Jr., T. Vreven, K.N. Kudin, J.C. Burant, J.M. Millam, S.S. Iyengar, J. Tomasi, V. Barone, B. Mennucci, M. Cossi, G. Scalmani, N. Rega, G.A. Petersson, H. Nakatsuji, M. Hada, M. Ehara, K. Toyota, R. Fukuda, J. Hasegawa, I.M. Ishida, T. Nakajima, Y. Honda, O. Kitao, H. Nakai, M. Klene, X. Li, J.E. Knox, H.P. Hratchian, J.B. Cross, C. Adamo, J. Jaramillo, R. Gomperts, R.E. Stratmann, O. Yazyev, A.J. Austin, R. Cammi, C. Pomelli, J.W. Ochterski, P.Y. Ayala, K. Morokuma, G.A. Voth, P. Salvador, J.J. Dannenberg, V.G. Zakrzewski, S. Dapprich, A.D. Daniels, M.C. Strain, O. Farkas, D.K. Malick, A.D. Rabuck, K. Raghavachari, J.B. Foresman, J.V. Ortiz, Q. Cui, A.G. Baboul, S. Clifford, J. Cioslowski, B.B. Stefanov, G. Liu, A. Liashenko, P. Piskorz, I. Komaromi, R.L. Martin, D.J. Fox, T. Keith, M.A. Al-Laham, C.Y. Peng, A. Nanayakkara, M. Challacombe, P.M.W. Gill, B. Johnson, W. Chen, M.W. Wong, C. Gonzalez, J.A. Pople, Gaussian, Inc., Wallingford CT, 2004.
[16] M. Cozi, G. Scalmani, N. Rega, V. Barone, J. Chem. Phys. 117 (2002) 43;
A. Pedone, J. Bloino, S. Monti, G. Prampolini, V. Barone, Phys. Chem. Chem. Phys. 12 (2010) 1000.
[17] S.F. Boys, F. Bernardi, Mol. Phys. 19 (1970) 553;
B. Liu, A.D. Mclean, J. Chem. Phys. 59 (1973) 4557;
H.B. Jansen, P. Ros, Chem. Phys. Lett. 3 (1969) 140.
[18] M.C. Diaz, B.M. Illescas, C. Seoane, N. Martin, J. Org. Chem. 69 (2004) 4492.
[19] T.L.J. Toivonen, T.I. Hukka, J. Phys. Chem. A 111 (2007) 4821.
[20] I.D. Petsalakis, I.S.K. Kerkines, N.N. Lathiotakis, G. Theodorakopoulos, Chem. Phys. Lett. 474 (2009) 278;
I.D. Petsalakis, N.N. Lathiotakis, G. Theodorakopoulos, J. Mol. Struct. (THEOCHEM) 867 (2008) 64.
[21] I.D. Petsalakis, N. Tagmatarchis, G. Theodorakopoulos, J. Phys. Chem. C 111 (2007) 14139.
[22] A. Sassara, G. Zerza, M. Chergui, F. Negri, G. Orlandi, J. Chem. Phys. 107 (1997) 8731.
[23] O. Christiansen, H. Koch, P. Jørgensen, Chem. Phys. Lett. 243 (1995) 409;
C. Hättig, A. Köhn, J. Chem. Phys. 117 (2002) 6939;
C. Hättig, F. Weigend, J. Chem. Phys. 113 (2000) 5154;
C. Hättig, J. Chem. Phys. 118 (2003) 7751;
A. Köhn, C. Hättig, J. Chem. Phys. 119 (2003) 5021.
[24] R. Ahlrichs, M. Bär, M. Häser, H. Horn, C. Kölmel, Chem. Phys. Lett. 162 (1989) 165;
R. Ahlrichs, M. Bär, M. Häser, H. Horn and C. Kölmel, TURBOMOLE, Version 5.10.
[25] I.D. Petsalakis, G. Theodorakopoulos, Chem. Phys. Lett. 466 (2008) 189;
G. Pagona, G. Rotas, I.D. Petsalakis, G. Theodorakopoulos, J. Fan, A. Maigne, M. Yadasaka, S. Iijima, N. Tagmatarchis, J. Nanosci. Nanotechnol. 7 (2007) 3468;
I.D. Petsalakis, G. Pagona, N. Tagmatarchis, G. Theodorakopoulos, Chem. Phys. Lett. 448 (2007) 115;
I.D. Petsalakis, G. Pagona, G. Theodorakopoulos, N. Tagmatarchis, M. Yudasaka, S. Iijima, Chem. Phys. Lett. 429 (2006) 194.
[26] X. Gao, S.B. Zhang, Y. Zhao, S. Nagase, Angew. Chem. 122 (2010) 6916;
X. Gao, S.B. Zhang, Y. Zhao, S. Nagase, Angew. Chem. Int. Ed. 49 (2010) 6764.